Available online at www.sciencedirect.com

ScienceDirect

Energy Procedia 45 (2014) 568 – 577

Energy Procedia

68th Conference of the Italian Thermal Machines Engineering Assbociation, ATI2013

Boundary Layer structure to derive marginal condition for spontaneous oscillations of a Thermoacoustic engine coupled with a piezoelectric element

Roberto Baccoli[1*], Costantino Mastino [1], Amr Baz[2].

1 University of Cagliari, Italy, Email: rbaccoli@unica.it*
2 University of Maryland 20742 College Park, Maryland, Email: baz@umd.edu

Abstract

This paper deals with the problem to derive a marginal condition for the onset of spontaneous thermoacoustic oscillations of a gas in a circular tube, subject to a variable shape of the temperature gradient along the side wall, with one end rigidly closed and the other closed by a piezoelectric element converter. In this study the acoustic impedance of the piezo element is arbitrary in order to achieve marginal conditions between those exhibited with rigidly closed end, and those with end opened onto free atmosphere. Moreover, marginal condition is outlined adopting a variable shape of the temperature gradient with respect to the position of the stack along the tube. The marginal condition is provided at the same time with respect to variable piezo-impedance and variable position of the acoustic driver. The solution includes all dissipative effects related to the compressive and shear viscosity and the heat transmission in the boundary layer at the side wall and end wall. The formulation is given in the framework of the linear theory and the first order theory in the ratio of a boundary layer thickness to the tube radius.

Keywords: thermoacoustics; marginal condition; boundary-layer theory

1. Introduction.

This study investigates one of the promising candidates in the field of energy conversion, namely a standing waves thermoacoustic engine. In thermoacoustic systems heat is converted into acoustic energy and vice versa. These systems use inert gases as a working medium and have no moving parts which makes the thermoacoustics technology a serious alternative to produce mechanical or electrical power, cooling power, and heating in a sustainable and environmentally friendly way. The experimental results up to present reveal a record performance of 49% of the Carnot efficiency for a thermoacoustic Stirling engine (see Tijania and Spoelstra [1]).

doi:10.1016/j.egypro.2014.01.061

Nomenclature

$p_e = p_0$	value of the uniform pressure related to the equilibrium state, [Pa];
T_e	local gas temperature in equilibrium conditions, [°C];
ρ_e	local gas density in equilibrium conditions, related to the local temperature T_e, [kg/m^3];
ν_e	kinematic viscosity, related to the local temperature T_e, [m^2/s];
a_e	local sound speed in equilibrium conditions, related to the local temperature T_e, [m/s];
c_v	specific heat capacity at constant volume of working fluid, [kJ/kg°C];
c_p	specific heat capacity at constant pressure of working fluid, [kJ/kg°C];
T_H	temperature at the hot, closed end, [°C];
T_0	temperature at the cold, open or piezo system mounted end, [°C];
γ	c_p/c_v;
Pr	Prandtl number;
$C = 1 + (\gamma - 1)/\sqrt{Pr}$;	$C_T = 1/2 + 1/\sqrt{Pr}$+Pr;
R	radius of the tube [m];
ω	angular frequency, [1/s]
ω	angular frequency, [1/s];
$\sigma = \frac{\omega L_T}{a_0}$	dimensionless angular frequency;
u_x	velocity in the axial direction, [m/s];
u_r	velocity in the radial direction, [m/s];
$\delta_e = \frac{1}{R}\sqrt{\frac{\nu_e}{i\omega}}$,	represent a measure of how is deep the boundary layer respect to the radius R
δ_0	δ_e calculated for $T = T_0$ at the low end wall temperature and C is a gas constant.
$b = C\,\delta_0$	frequency equation (21) is obtained in the zero and in the first order by expanding the wave perturbed pressure equation with respect to *b*;
i	imaginary part;
$x_p \in [-L_*, +L_p]$	("p" region) domain were the temperature gradient is negative and characterized by a slow slope. Quantities are designated by attaching a subscript "p" (e.g. T_{ep}, T_p', $\tilde{T}_p$);
L_p	abscissa at the end wall where is placed the piezo-system converter. The temperature in this point is the lowest one and is indicated by T_0;
$x_n \in [-L_n, -L_*]$	("n" region) domain were the temperature gradient is negative and characterized by an high slope. Quantities are designated by attaching a subscript "n" (e.g. T_{en}, T_n', $\tilde{T}_n$);
$-L_n$	abscissa value that localize the position of the end wall resonator respect to the origin of the system reference. The temperature in this point is the highest one and is indicated by T_H;
$L_T = L_n + L_p$	length of the tube, [m];
$-L_*$	abscissa value that localize the point where the slope of the temperature gradient changes dramatically his value and $T_e(-L_*)$ is equal to T_*;
λ_p	is a parameter that governs the magnitude and the sign of the slope of the temperature gradient in the "p" region so that $\frac{a_{ep}}{T_{ep}}\frac{dT_{ep}}{dx_p} = 2\frac{a_0\lambda_p}{L_p}$;
λ_n	is a parameter that governs the magnitude and the sign of the slope of the temperature gradient in the "n" region so that $\frac{a_{en}}{T_{en}}\frac{dT_{en}}{dx_n} = 2\frac{a_0\lambda_n}{L_n}$;
$U_p = i\frac{2C_T}{C} b e^{-\frac{\lambda_p}{L_p}\xi_p^*}\lambda_p\left(\frac{L_T}{L_p\sigma}\right)^2\psi_p$;	$I_p = 1 + i\frac{2C_T}{C} b e^{-\frac{\lambda_p}{L_p}\xi_p^*}\lambda_p\left(\frac{L_T}{L_p\sigma}\right)^2\frac{i\lambda_p}{2}$;
$g = (1-(1+\lambda_n)b)(1+\lambda_n)$;	$d = \frac{2C_T}{C}\lambda_n(1+\lambda_n)b$;
$J = \frac{kr\cdot\sigma^2}{L_n\cdot(1+\lambda_n)^2(1-2\cdot(1+\lambda_n))\cdot\frac{b}{C}}$ where kr is a parameter that governs the volume size of the resonator cavity	

* Corresponding author. Tel.: +39 0706755262; fax: +39 0706755263
E-mail address rbaccoli@unica.it

Literature includes several mathematical models for integrating the engine with a piezoelectric membrane generator to obtain a thermoacoustic-piezo system (TAP), distinct among these studies are recent results from Smoker and Baz. [2], and Nouh and Baz [3]. In this paper, an attempt is made to provide a preparatory contribution in order to develop an optimization tool for piezoelectric element coupled with a thermoacoustic engine as a function of piezoelectric impedance and also of the shape of the temperature trend along the tube's wall. A configuration of the system under study is shown in figure 1

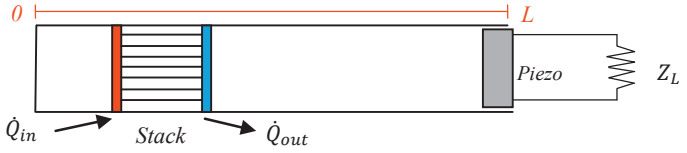

Figure 1. Schematic of standing-wave thermoacoustic engine integrated with a piezoelectric membrane (TAP)

Thermoacoustics has attracted much attention over the past few decades from the viewpoint of its potential in application to novel heat engines and cooling systems.

Although such phenomena have been known empirically or experimentally since 19th century (see Rayleigh [4]), no analysis of stability was made until the pioneering works started by Kramers [5] (1949) and Rott [5] (1969).

They attempted to seek a marginal condition for the onset of the Taconis oscillations (see Taconis et al. [6]) in a helium-filled tube in cryogenics. Although Kramers failed, Rott succeeded in deriving the conditions, which are confirmed experimentally by Yazaki, Tominaga et Al. [7]. Since then, Rott's linear theory has played a fundamental role and has been applied to design experimental devices**.**

The right theoretical frame in order to get the marginal condition was derived by Rott [5] [8] [9] and afterwards it was completed by Wheatley [10] and Swift [11]. Rott's works are about quarter wave length tube. The linearized problem requires to solve an eigenvalue problem for a second-order differential equation with variable coefficients in terms of the excess pressure wave. For smooth temperature distributions, this is a formidable task and, apart the excellent Sugimoto's work, no analytical solutions are available yet.

Indeed Rott gave up the smooth profile of the temperature and adopted a discontinuous trend, namely a heaviside function, thereby imposing a drastic discontinuity, though it is rather difficult to achieve experimentally. In 2001, the excellent work of Sugimoto et al [12], shed some light on what happens on the onset of thermoacoustic oscillations. Thanks to his work was discovered the mechanism whereby the boundary layer, under an appropriate temperature gradient, is able to supply a work to the wave pressure propagation up to exceed dissipative effects of the viscous boundary layer.

This would mean that the sustenance of wave propagation in the axial direction, inside the main flow, is ensured by the boundary layer itself and, thanks to the temperature gradient along the direction of propagation, it is in conditions to provide the necessary work compensation, up to exceeding the dissipative effects. As a further development, starting from a problem having a boundary layer structure, in Sugimoto et al [13] has been found an exact solution for the excess pressure wave in the acoustic main flow region. The solutions are given in terms of analytical approximation of the full solution through a perturbation expansion, using a renormalization. Sugimoto's work deals with only the case where the temperature increases parabolically from the open end, toward the closed end as show in figure 2.

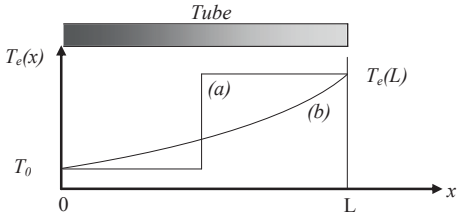

Figure 2. Illustration of a quarter – wave length tube of radius R and of length L where the temperature of the wall and the gas Te(x) varies along the tube in the form of a heaviside (a) function and of a parabola (b)

In what follows, this work adopts the Sugimoto's approach with only two minor extensions with the aim to offer two points of generalization. The first one is related to the boundary condition at one end, because the complex value of the piezoelectric impedance is taken into account, and the second effort is about the possibility to build a variable shape of temperature gradient by means of a sequence of piecewise parabolic distribution as shown in figure 3.

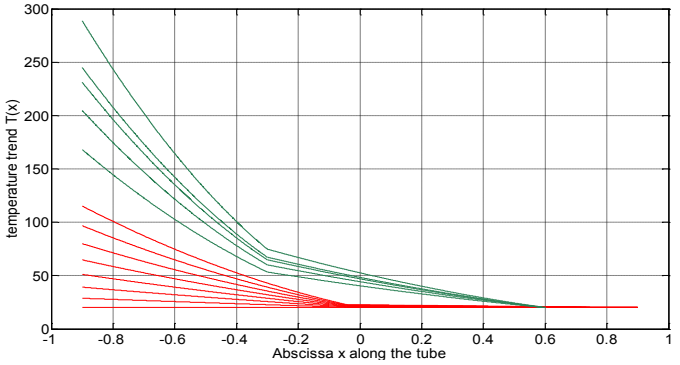

Figure 3. Some examples of the shape of the temperature imposed along the tube in stationary conditions. The aim is to investigate the behaviour of the marginal condition when the shape goes towards the real temperature distribution inside the resonator.

2. A problem with a Boundary Layer structure: the main lossless flow and the viscous - thermal boundary layer

Here, we assume that the field of the acoustic flow has a boundary layer structure, which means that the influence of viscosity is confined to a thin layer near the wall. The flow is basically divided in a boundary layer region and the flow outside of it, namely the main flow. The latter is where the effects of non-linearity and dissipation due to viscosity and heat transmission are very small, such that it can be neglected and quasi one dimensional propagation can be assumed. Regarding the former region, it is necessary to take into account two boundary layer regions: one that is placed on the side wall, along the length of the tube, where viscous effect are more predominant than the thermal ones (basically it is a viscous boundary layer), and another one on the end wall, mainly due to heat transmission, since there the boundary temperature of the main flow does not match directly with the temperature of the end wall. In fact, it is necessary that a thermal boundary layer fills the gap (instead the viscous boundary layer plays a secondary role respect to the thermal one), see Chester [14], Chester [15].
The small deviations from the equilibrium value are designated by attaching a tilde accent, $\widetilde{\varphi}$, and by a grave one, $\grave{\varphi}$, according to whether it is considered the boundary layer of the side wall or that of the end wall, respectively.

An abscissa x parallel to the axis of the tube, is adopted to establish a spatial reference for the main flow region, moreover x coupled with a transversal coordinate, $n_{\perp}$, represents a spatial reference for the boundary layer at side wall, while with $n_{\parallel}$, oriented in the axial direction, is designated as a reference related to the boundary layer at the end wall. Reassuming:
$n_{\perp}$ denotes the boundary layer coordinate taken inward normal to the tube wall surface at r =R, whereas $n_{\parallel}$ denotes the boundary layer coordinate taken inward normal to the end wall at x=L. In accordance with our previous statements it follows:

$\varphi = \varphi_e(x) + \varphi'(x,t)$ is referred to the main flow
$\varphi = \varphi_e(x) + \grave{\varphi}(n_{\parallel},t)$ is referred to the boundary layer at the end wall
$\varphi = \varphi_e(x) + \widetilde{\varphi}(x,n_{\perp},t)$ is referred to the boundary layer at the side wall

The basic equations governing the motion of a fluid are the axial and radial momentum equations, the continuity equation, the energy equation and the equation of state. For a perfect gas with constant specific heats c_p and c_v, constant dynamic shear and bulk viscosity μ, μ_v, and constant heat conductivity λ, due to cylindrical symmetry phenomena, become respectively, (see eq (1-5)):

$$\frac{\partial \varrho}{\partial t} + \left[\frac{1}{r}\frac{\partial (r\varrho u_r)}{\partial r} + \frac{\partial (\varrho u_x)}{\partial x}\right] = 0 \tag{1}$$

$$\varrho\left(\frac{\partial u_x}{\partial t} + u_r\frac{\partial u_x}{\partial r} + u_x\frac{\partial u_x}{\partial x}\right) = -\frac{\partial p}{\partial x} + \left(\frac{1}{3}\mu + \mu_v\right)\frac{\partial}{\partial x}\left[\left(\frac{1}{r}\frac{\partial (ru_r)}{\partial r} + \frac{\partial u_x}{\partial x}\right)\right] + \mu\left[\frac{1}{r}\frac{\partial}{\partial r}\left(r\frac{\partial u_x}{\partial r}\right) + \frac{\partial^2 u_x}{\partial x^2}\right] \tag{2}$$

$$\varrho\left(\frac{\partial u_r}{\partial t} + u_r\frac{\partial u_r}{\partial r} + u_x\frac{\partial u_r}{\partial x}\right) = -\frac{\partial p}{\partial r} + \left(\frac{1}{3}\mu + \mu_v\right)\frac{\partial}{\partial r}\left[\left(\frac{1}{r}\frac{\partial (ru_r)}{\partial r} + \frac{\partial u_x}{\partial x}\right)\right] + \mu\left[\frac{1}{r}\frac{\partial}{\partial r}\left(r\frac{\partial u_r}{\partial r}\right) + \frac{\partial^2 u_r}{\partial x^2}\right] \tag{3}$$

$$\varrho T\left(\frac{\partial s}{\partial t} + u_r\frac{\partial s}{\partial r} + u_x\frac{\partial s}{\partial x}\right) = \lambda\left[\frac{1}{r}\frac{\partial}{\partial r}\left(r\frac{\partial T}{\partial r}\right) + \frac{\partial^2 T}{\partial x^2}\right] + \phi \tag{4}$$

where φ is the so called viscous dissipative function, such that:

$$\phi = 2\mu\left[\left(\frac{\partial u_r}{\partial r}\right)^2 + \left(\frac{u_r}{r}\right)^2 + \left(\frac{\partial u_x}{\partial x}\right)^2\right] + \mu\left(\frac{\partial u_r}{\partial x} + \frac{\partial u_x}{\partial r}\right)^2 + 2\left(\mu_v - \frac{2}{3}\mu\right)\left(\frac{1}{r}\frac{\partial (ru_r)}{\partial r} + \frac{\partial u_x}{\partial x}\right)^2 \tag{4.1}$$

$$\frac{p}{p_0} = \left(\frac{\varrho}{\varrho_0}\right)^{\gamma} e^{\left(\frac{s-s_0}{c_v}\right)} \tag{5}$$

See Nomenclature for the meaning of the symbols used throughout in the paper. We start by assuming that all the perturbed quantities are related, respect to their equilibrium value, by these order relations:

$$\varphi'(x,t), \qquad \dot{\varphi}(n_{\parallel},t,), \qquad \tilde{\varphi}(x,n_{\perp},t) \ll \varphi_e(x)\,;$$

If these inequalities are true, then the framework of the mathematical interpretation of the phenomena is based on the small signal approximation namely the linearization of all the conservation equation.

3. Treatment of the acoustic main flow.

The linearized main flow equations around equilibrium values, when lossless and quasi-one dimensional flow is considered, and subsequently on averaging over the whole cross sectional area, yields respectively:

$$\varrho_e\frac{\partial u_x}{\partial t} = -\frac{\partial p'}{\partial x} \tag{6}$$

$$\frac{\partial \varrho'}{\partial t} + \frac{\partial \varrho_e u_x}{\partial x} - \frac{1}{A}\oint_{\partial A}\varrho_e\frac{\partial u_r}{\partial r}da = 0 \tag{7}$$

where A(x, t) is the cross-sectional area of the main-flow region and it is both time and "x" dependent, but no distinction from the constant cross-sectional area of the tube itself will be considered, because the difference is small and of an higher order. The integral is taken along ∂A, namely the cross section boundary of the main flow region, "*da*" being a line element along it. Remark: $\text{at } \partial A \;\; r \cong R \text{ then } \frac{1}{r}\frac{\partial (ru_r)}{\partial r} \cong \frac{\partial u_r}{\partial r}$

$$\varrho\left(\frac{\partial u_x}{\partial t}\right) = -\frac{\partial p'}{\partial x} + \left(\frac{4}{3}\mu + \mu_v\right)\frac{\partial^2 u_x}{\partial x^2} \tag{8}$$

$$\varrho_e T_e u_x\frac{\partial s_e}{\partial x} + \varrho_e T_e\frac{\partial s'}{\partial t} = \lambda\frac{\partial^2 T'}{\partial x^2} \tag{9}$$

$$\frac{T'}{T_e} = (\gamma - 1)\frac{\varrho'}{\varrho_e} + \frac{s'}{c_v} \tag{10}$$

4. Treatment of the Acoustic Boundary Layer Regions.

In agreement with what was derived by Sugimoto in [13] and Lighthill in [16], the governing equations of continuity, momentum in the axial direction, and the energy balance, with dissipative effects fully taken into account, linearized around the steady state value $(\varrho_e, T_e, p_0, S_e)$, yields the following equations (11-13):

4.1 Boundary Layer at the side wall.

$$\frac{\partial \tilde{\varrho}}{\partial t} + \left[\frac{\partial(\varrho_e \tilde{u}_x)}{\partial x} + \frac{\partial(\varrho_e \tilde{u}_r)}{\partial n_\perp}\right] = 0 \tag{11}$$

$$\varrho_e \frac{\partial \tilde{u}_x}{\partial t} = -\frac{\partial \tilde{p}}{\partial x} + \mu \frac{\partial^2 \tilde{u}_x}{\partial {n_\perp}^2} \tag{12}$$

$$\varrho_e T_e \left(\frac{\partial \tilde{s}}{\partial t} + \tilde{u}_x \frac{\partial s_e}{\partial x}\right) = \lambda \left[\frac{\partial^2 \tilde{T}}{\partial {n_\perp}^2}\right] \tag{13}$$

Remark: inside the boundary layer region $R - n_\perp \cong R$ then $\frac{1}{R-n_\perp}\frac{\partial((R-n_\perp)(\circ))}{\partial n_\perp} \cong \frac{\partial(\circ)}{\partial n_\perp}$

4.2 Boundary Layer at the end wall

$$\frac{\partial \dot{\varrho}}{\partial t} + \frac{\partial(\varrho_e \dot{u}_x)}{\partial n_\parallel} = 0 \tag{14}$$

$$\varrho_e \frac{\partial \dot{u}_x}{\partial t} = -\frac{\partial \dot{p}}{\partial n_\parallel} + \left(\frac{4}{3}\mu + \mu_v\right)\frac{\partial^2 \dot{u}_x}{\partial {n_\parallel}^2} - \mu \oint_{\partial A} \frac{\partial \dot{u}_x}{\partial n_\perp} \tag{15}$$

$$0 = -\frac{\partial \dot{p}}{\partial r} \tag{16}$$

$$\varrho_e T_e \left(\frac{\partial \dot{s}}{\partial t} + \dot{u}_x \frac{\partial s_e}{\partial x}\right) = \lambda \left[\frac{\partial^2 \dot{T}}{\partial {n_\parallel}^2}\right] - \lambda \oint_{\partial A} \frac{\partial \dot{T}}{\partial n_\perp} \tag{17}$$

Once the governing equations of the boundary layer on the end wall have been linearized, are subsequently also averaged over the whole cross section with area $A_0 (= \pi R^2)$.

Contrarily to what happens for the walls placed parallel to the main flow direction, the modifications caused by wall oriented perpendicular are mainly assumed by the main flow, while the effects related to the viscous boundary layer are almost negligible. In accordance with what we said before this can only apply to viscous effect but is not true for the thermal boundary layer. By using the two system of equations regarding the main flow and the boundary layer on the side wall, it is possible to write down equation (18); that is a second order differential equation with variable coefficients of the axial coordinate "x" involving the Fourier transform "*P*" of the excess pressure p', in the main-flow region.

$$(1 - 2C\delta_e)a_e^2 \frac{d^2P}{dx^2} + [1 - 2(C + C_T)\delta_e]\frac{a_e^2}{T_e}\frac{dT_e}{dx}\frac{dP}{dx} + \omega^2 P = 0 \tag{18}$$

whereas the boundary layer equations on the two ends wall of the tube are taken into account in the form of an appropriate boundary conditions customized for the main flow region. Equation (18) has been proposed by Sugimoto, (see eq. 23 in [13]) and it was used to get the stability analysis for the marginal conditions.

5. Boundary conditions at the ends wall of the tube.

When the tube is rigidly closed at one end and open on the other side, the boundary conditions for the main flow are well known, namely:

$$\left(\frac{dp'}{dx} = -\frac{\gamma-1}{\sqrt{Pr}}\frac{\sqrt{\nu_L}}{a_L^2}\frac{d^{3/2}p'}{dt^{3/2}}\right)_{x=0} \qquad \text{at the closed end}$$

$$(p' = 0\,)_{x=L_p} \qquad \text{at the opened end.}$$

where the derivative of three and half order is defined by differentiating that of half order once with respect to t, and the fractional derivatives of order α (α = −1/2 or 1/2) of a function f(x; t) are defined as (see e.g. Sugimoto [17])

$$\frac{d^{\alpha}\oint}{dt^{\alpha}} = -\frac{1}{\pi}\int_{-\infty}^{t}\frac{1}{\sqrt{t-\tau}}\frac{\partial^{\alpha+1/2}}{d\tau^{\alpha+1/2}}\oint(x,t)d\tau$$

By using the idea of a renormalization of eq. (18) and in the framework of the first-order theory of the boundary layer, the frequency equation is then derived from the boundary conditions at the both ends of the tube when the temperature distribution is parabolic, from which the marginal condition, eq. (19), is obtained in closed form, in terms of the dimensionless angular frequency, $\sigma = \frac{\omega L}{a_0}$, as a function of the ratio, T_H/T_0, of temperature at the hot, closed end, $T_H=T_e(x=L)$, to the one at the cold, open end, $T_0=T_e(x=0)$, against the tube radius relative to the thickness of the boundary layer at the open end:

$$i\psi\left(\frac{e^{iK^+\xi_L}+e^{iK^-\xi_L}}{e^{iK^+\xi_L}-e^{iK^-\xi_L}}\right) = \frac{\beta}{2} - \frac{2C_T}{C}\beta b + \left(1-\frac{1}{C}\right)\frac{R}{L}\sigma^2 b \qquad (19)$$

where β is a parameter that sets the slope of the parabola:
$\frac{T_e(x)}{T_0} = \left(1+\beta\frac{x}{L}\right)^2$; K^+, K^- are the wave-numbers and they are given by: $K^{\pm}L = -\frac{i}{2}\beta \pm \psi$ with $\psi = \sqrt{\sigma^2 - \frac{\beta^2}{4}}$. For a given value of β the frequency equation gives a complex solution for σ. If the imaginary part is positive the oscillations are stable, if it is negative, they are unstable. The marginal condition is the one for which the imaginary part goes to zero. In figure 4 is shown the solution of the angular frequency σ against the temperature ratio T_H/T_0, for the marginally unstable oscillations of air. The solid curve shows the frequency of the neutral oscillations in the lossless case, as the magnitude of the thermoviscous effects increases, the value of sigma and temperature ratio decreases along the solid curve, but tends to deviate from the lossless trend

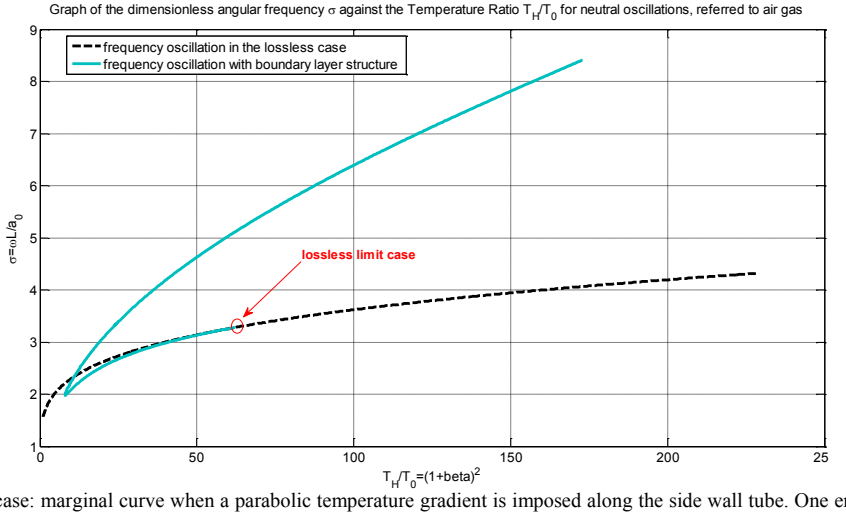

Figure 4. Sugimoto's case: marginal curve when a parabolic temperature gradient is imposed along the side wall tube. One end is opened and the other is rigidly closed. The curve represented in dashed lines is adopted for lossless case, whereas continuous is referred when loss are taken into account.

6. New boundary conditions

The effort of this work is to get new boundary conditions when the tube is rigidly closed at one end and at the other side is closed by means of a piezoelectric element with a variable impedance and the side wall is subject to a variable shape of the temperature. Equation (20) and (21), in the frequency domain, respectively represent the new boundary condition in x=L_p, where piezoelectric element is placed and the Sugimoto's boundary condition in x=0 where end wall is rigidly closed.

$$\left(\frac{dP}{dx} = -\frac{1+G(Z_{piezo})^{-1}}{G} i\omega Q_L P\right)_{x=L_p} \tag{20}$$

where $\frac{1}{G} = \frac{\gamma-1}{\sqrt{Pr}}\frac{1}{{a_0}^2}\sqrt{i\omega\nu_L}i\omega P$ and $z_{piezo} = \frac{\mathcal{F}\{p'\}}{\mathcal{F}\{u_x'\}}$ is the impedance of the piezoelectric system.

$$\left(\frac{dP}{dx} = -\frac{\gamma-1}{\sqrt{Pr}}\frac{\sqrt{\nu_L}}{{a_0}^2}\sqrt[2]{i\omega^3}P\right)_{x=0} \tag{21}$$

When Z_{piezo} goes to ∞ (referred to the physical condition where end wall is rigidly closed) the new boundary condition converges just to the previous one, in accordance with Sugimoto et al. [13]. While if Z_{piezo} goes to zero (that physically corresponds to open end) then eq. (20) converges rightly to p'= 0. The new frequency equation, eq. (21), is derived by using the boundary layer equation between the piezoelectric element and the main flow region, when the temperature distribution is variable as shown in figure 3.

$$\log\frac{\eta_{L_n}}{\eta_p^*} + b\left(\eta_{L_n} - \eta_p^*\right)\frac{\lambda_n}{4\psi_n}\log\left\{\frac{\left[\left(\frac{\lambda_n}{2L_n}+\frac{i\psi_n}{L_n}\right)W+g\cdot J\right]\left\{\left[(B+P)V_s+(D-A)i\psi_p\right]\left[e^{iKp\xi_p^*}+e^{i\ell p\xi_p^*}\right]+\left[(A-D)V_s-(B+P)i\psi_p\right]\left[e^{iKp\xi_p^*}-e^{i\ell p\xi_p^*}\right]\right\}}{\left[\left(\frac{\lambda_n}{2L_n}-\frac{i\psi_n}{L_n}\right)W+g\cdot J\right]\left\{\left[BV_s-Ai\psi_p\right]\left[e^{iKp\xi_p^*}+e^{i\ell p\xi_p^*}\right]+\left[AV_s-Bi\psi_p\right]\left[e^{iKp\xi_p^*}-e^{i\ell p\xi_p^*}\right]\right\}}\right\} = 0 \tag{22}$$

Quantities in equation (21) not defined yet, are explained in appendix A.

A set of marginal curves in the loss case, as a function of the piezo-impedance, and the shape of the temperature trend (in terms of L_* and L_p) is depicted in figures 5, 6 and 7.

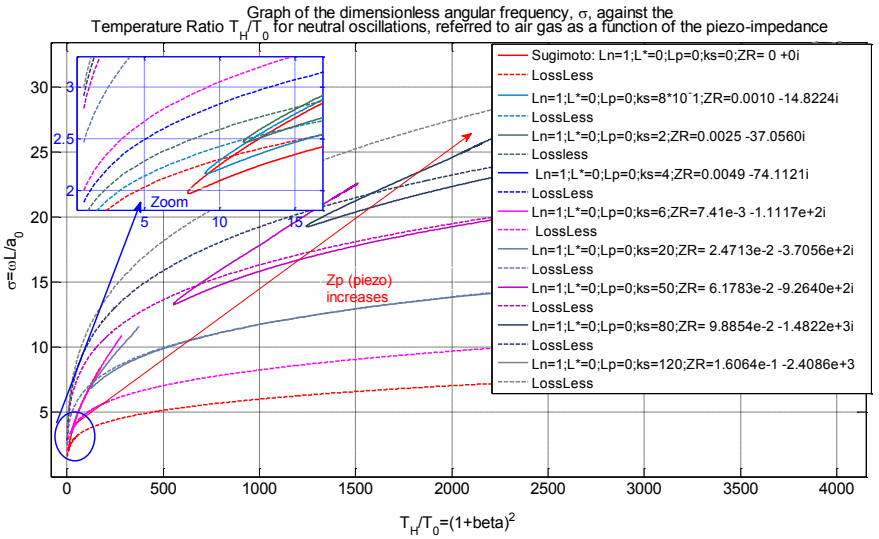

Figure 5. Marginal curve when a parabolic temperature gradient is imposed along the side wall tube. One end is opened and the other is closed by a piezo-electric element. The acoustic impedance of the piezo-element is arbitrary in order to achieve marginal conditions between those exhibited with rigidly closed end, and those with end opened to free atmosphere.

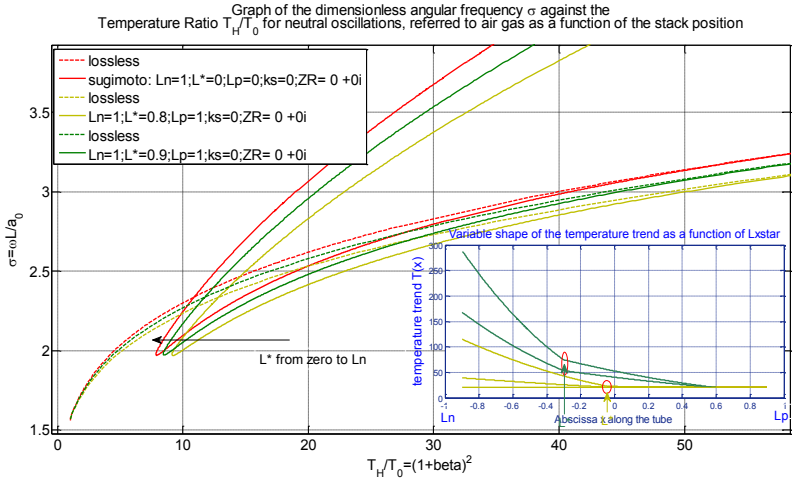

Figure 6. Marginal curve when the temperature trend is stretched due to different position of the stack, (L_* is different from zero). The curve represented in dashed lines is adopted for lossless case, whereas continuous is referred when loss are taken into account. One end is opened and the other is closed by a piezo-electric element with its impedance equal to zero.

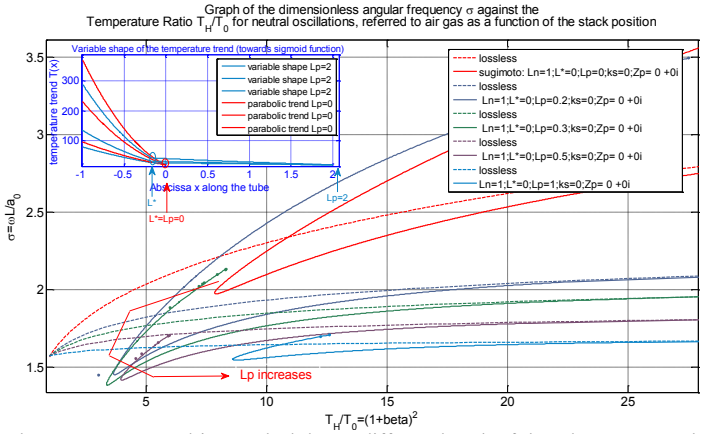

Figure 7 Marginal curve when the temperature trend is stretched due to different length of the tube respect to the position of the stack, (L_p is different from zero). The curve represented by dashed lines is for the lossless case, whereas the continuous line is referred when loss are taken into account. One end is opened and the other is closed by a piezo-electric element with its impedance equal to zero.

7. Conclusion

In accordance with what was said before in this work the main improvements to the best of our knowledge are summarized below.

We found an analytical solution for the marginal conditions as a function of the value of the impedance of the piezoelectric element placed at the end wall of the tube. This solution is not only limited to the boundary conditions of opened and rigidly closed end.

The shape of the temperature gradient along the axial direction of the tube is variable and it is possible to realize changes where the slope is able to approximate at best the real temperature trends, as a function of the position of the stack along the tube and its length.

Based on the shape of the temperature gradient and the impedance of the piezoelectric element it is possible to determine the minimum threshold value for the temperature gradient required for the onset of oscillations.

Thanks to the flexibility of our model it is possible to get a theoretical prediction in order to match the resonant frequencies with the temperature ratio as a function of the electric load.

References

[1] Tijania M E H, Spoelstra S. "A high performance thermoacoustic engine", Journal of Applied Physics 110, 093519 (2011)
[2] Nouh M, Aldraihem O, Baz A. "Energy Harvesting of Thermoacoustic-piezo Systems with a Dynamic Magnifier", ASME Journal of Vibration & Acoustics, Vol. 134, No. 4, 061015, Dec. 2012.
[3] Smoker J, Nouh M, Aldraihem O, and Baz A. "Energy harvesting from a standing wave thermoacoustic-piezoelectric resonator", Journal of Applied Physics, Vol.111, No. 10, 16 May 2012.
[4] Lord Rayleigh, The Theory of Sound _Dover, New York, 1945_, Vol. 2, pp. 230–231.
[5] Kramers H. A. "Vibrations of a gas column," Physica Amsterdam, 15, 971 1949
[6] Taconis K W, Beenakker J J M, Nier A O C, Aldrich L T. "Measurements concerning the vapour-liquid equilibrium of solutions of He3 in He4 below 2.19 K," Physica _Amsterdam_ 15, 733 _1949_.
[7] Yazaki T, Iwata A, Maekawa T, Tominaga A. "Traveling wave thermoacoustic engines in a looped tube" Phys. Rev. Lett. 81, 3128 1998.
[7] Rott N. ''Damped and thermally driven acoustic oscillations in wide and narrow tubes,'' Z. Angew. Math. Phys. 20, 230–243 (1969).
[8]Rott N. "Thermally Driven Acoustic Oscillations. Part II: Stability Limit for Helium" Journal of Applied Mathematics and Physics (ZAMP) Vol. 24, 1973
[9] Rott N. "Thermally Driven Acoustic Oscillations, Part V Gas-Liquid Oscillations" Journal of Applied Mathematics and Physics (ZAMP) Vol. 27, 1976
[10] Wheatley J. C. "Intrinsically irreversible or natural engines," in Frontiers in Physical Acoustics, edited by D. Sette North Holland, Amsterdam, 1986_, pp. 9395–475.
[11] Swift G. W. "Thermoacoustic engines," J. Acoust. Soc. Am. 84, 1145 1988.
[12] Sugimoto N, Tsujimoto K. "Amplification of energy flux of nonlinear acoustic waves in a gas-filled tube under an axial temperature gradient", J. Fluid Mech. vol. 456, pp. 377-409, (2002),
[13] Sugimoto N,Yoshida M. "Marginal condition for the onset of thermoacoustic oscillations of a gas in a tube" Phys. Fluids 19, 074101 (2007); doi: 10.1063/1.2742422.
[14] Chester, W. "Resonant oscillations in closed tubes," JFM, 18, No. I, 44-64 (1964).
[15] Chester, W."Resonant Oscillations of Water Waves. I. Theory", proc. Roy. Soc. 306, 5-22 (1968).
[16] Lighthill, M. J. "Surveys in Mechanics" (edited by G. K. Batchelor & R. M. Davies) 1956.
[17] Sugimoto N. "Generalized Burgers equations and fractional calculus", in Nonlinear Wave Motion (A. Jeffrey, Ed.), pp. 162_179, Longman Scientific, Harlow, 1989.

Appendix A

Hereafter are listed all quantities that appear explicitly in eq. (21).

$$\eta_p^* = \eta_p(-L_*) = 1 + \lambda_p = \sqrt{\frac{T_*}{T_0}}; \qquad \eta_{L_n} = \eta_n(-L_n) = \sqrt{\frac{T_*}{T_0}} - \frac{\lambda_n}{L_n}(-L_n + L_*) = \sqrt{\frac{T_H}{T_0}};$$

$$\xi_p^* = -\frac{L_p}{\lambda_p}\left(\log\eta_p - b\,\lambda_p\right); \qquad h = i \cdot e^{-\frac{C}{\sigma R}\sqrt{\frac{\nu_0 L_T}{2a_0}}\lambda_p} \cdot e^{i\frac{C}{\sigma R}\sqrt{\frac{\nu_0 L_T}{2a_0}}\lambda_p} \cdot \frac{2C_T}{C} b\lambda_n \left(\frac{L_T}{L_n\sigma}\right)^2;$$

$$R_n = 1 + i\frac{2C_T}{C}\lambda_n \frac{e^{-\frac{\lambda_n}{L_n}\xi_n^*}}{L_n K_n}; \qquad \psi_p = \sqrt{\left(\frac{\lambda_p}{2}\right)^2 - \left(\frac{L_p\sigma}{L_T}\right)^2}; \qquad K_p = \frac{1}{L_p}\left(-i\frac{\lambda_p}{2} + \psi_p\right);$$

$$\ell_p = \frac{1}{L_p}\left(-i\frac{\lambda_p}{2} - \psi_p\right); \qquad G_n = 1 + i\frac{2C_T}{C}\lambda_n \frac{e^{-\frac{\lambda_n}{L_n}\xi_n^*}}{L_n \ell_n}\psi_p; \qquad W = \frac{1 - g\cdot d\cdot J\cdot (L_T)^2}{L_n\cdot\sigma^2};$$

$$X_{n,p} = i\frac{\lambda_{n,p}}{L_{n,p}}; \qquad Y_{n,p} = \frac{\psi_{n,p}}{L_{n,p}}; \qquad S = \frac{\mathrm{L_{po}}\varrho_0\omega}{Z_{piezo}} \qquad B = -\left(\frac{U_p}{R_n} + \frac{G_n L_n}{2\psi_n}\left(Y_p - \frac{U_p(X_n+Y_n)}{R_n}\right)\right);$$

$$P = \frac{U_p}{R_n} - L_n h\left(Y_p - \frac{U_p(X_n+Y_n)}{R_n}\right); \quad A = \frac{I_p}{R_n} - \frac{G_n L_n}{2\psi_n}\left(X_p - \frac{I_p(X_n+Y_n)}{R_n}\right); \quad D = \frac{I_p}{R_n} - L_n h\left(X_p - \frac{I_p(X_n+Y_n)}{R_n}\right);$$

$$V_s = \frac{\lambda_p}{2} + S - S\cdot b + \mathrm{L_p}\cdot T\frac{\sigma^2}{L_T}b; \qquad \psi_p = V_s - \frac{1}{2}\cdot S\cdot b\cdot(1-b)\cdot\frac{2C_T}{C}\cdot\left(\frac{\lambda_p L_T}{\mathrm{L_p}\sigma}\right)^2$$